Quercetin-3-O-α-L-rhamnopyranoside derived from the leaves of *Lindera aggregata* (Sims) Kosterm. evokes the autophagy-induced nuclear factor erythroid 2-related factor 2 antioxidant pathway in human umbilical vein endothelial cells

HAOTE HAN[1,2], BO XU[3], AWAIS AMIN[1,2], HONGLIANG LI[1,2], XIUYING YU[1,2], MINGHUA GONG[4] and LIN ZHANG[1,2]

[1]Department of Biomedical Engineering, Zhejiang University; [2]Zhejiang-Malaysia Joint Research Center for Traditional Medicine, Zhejiang University, Hangzhou, Zhejiang 310027; [3]Shandong Provincial Hospital Affiliated to Shandong University, Jinan, Shandong 250355; [4]Changshu Research Institute of Zhejiang University, Changshu, Jiangsu 215500, P.R. China

Received March 8, 2018; Accepted August 24, 2018

DOI: 10.3892/ijmm.2018.3976

Abstract. Quercetin-3-O-α-L-rhamnopyranoside (QI) is derived from the leaves of *Lindera aggregata* (Sims) Kosterm. And exhibits multiple biological activities, including an antioxidant activity. However, the detailed molecular mechanism of its antioxidant activity remains unknown. The aim of the present study was to investigate the antioxidant activity of QI and the underlying molecular mechanism in human umbilical vein endothelial cells (HUVECs). An oxidative stress model was established in HUVECs using H_2O_2, and cells were then treated with different concentrations of QI. The results revealed that the exposure of HUVECs to QI protected these cells from H_2O_2-induced damage. QI treatment also increased the activities of the antioxidant enzymes superoxide dismutase (SOD) and glutathione (GSH) in the cell culture medium. In addition, QI inhibited H_2O_2-induced apoptosis by decreasing the expression levels of cleaved Caspase-9 and poly(ADP-ribose) polymerase. QI also inhibited the production of DNA fragments and reactive oxygen species induced by H_2O_2. Furthermore, QI decreased the oxidative stress by promoting the nuclear transfer of nuclear factor erythroid 2-related factor 2 (Nrf2) and heme oxygenase-1 by activating autophagy, and inhibited the competition of Bach1 from Nrf2. Finally, QI significantly improved the activities of T-SOD and GSH, and decreased the content of malondialdehyde in the serum and heart tissue of aging rats. These data support the use of QI as a health supplement to alleviate oxidative stress or further development of this compound as an antioxidant drug.

Correspondence to: Dr Lin Zhang, Department of Biomedical Engineering, Zhejiang University, 148 Tianmushan Road, Hangzhou, Zhejiang 310027, P.R. China
E-mail: zhanglin@zju.edu.cn

Key words: Quercetin-3-O-α-L-rhamnopyranoside, human umbilical vein endothelial cells, oxidative stress, nuclear factor erythroid 2-related factor 2, autophagy

Introduction

Oxidative stress is involved in the pathogenesis of lifestyle-associated diseases, including atherosclerosis, hypertension, diabetes mellitus, ischemic diseases and malignancies (1). Oxidative stress results from an imbalance in pro-oxidant/antioxidant homeostasis that leads to the generation of toxic reactive oxygen species (ROS), such as hydrogen peroxide, organic hydroperoxides, nitric oxide, superoxide and hydroxyl radicals (2). Excessive free radicals in the body attack proteins, lipids, DNA and other biological macromolecules, leading to damaged cell structures, interference with normal metabolic activity, disease and accelerated aging (3). Thus, reducing oxidative stress is both indispensable and significant in improving the quality of life and treatment options for patients with oxidative stress-associated diseases. Due to the potential health hazards of synthetic antioxidants, such as dibutyl hydroxyanisole, which is carcinogenic in animal models, searching for efficient natural antioxidants from plants with low toxicity is of utmost importance in the development of safe antioxidants.

The Kelch-like ECH-associated protein 1 (Keap1)/nuclear factor erythroid 2-related factor 2 (Nrf2) signaling pathway is essential for cytoprotection against oxidative stress. Nrf2 is a potent transcriptional activator that serves a central role in the expression of numerous cytoprotective genes in response to oxidative stress (4). BTB and CNC homolog 1 (Bach1) is a transcription factor that functions as an Nrf2 repressor, competing with Nrf2 to downregulate the expression of antioxidant enzymes, and thus serving an important role in the regulation of the body's oxidant/antioxidant imbalance (5). The cellular oxidative stress induced by H_2O_2 shares the biological and morphological characteristics of apoptosis (6). However,

since oxidative damage varies clinically and is not permanent, the effects of oxidative stress cannot be solely explained by apoptosis. Under stress conditions, such as nutrient deprivation, oxidative stress and/or metabolic stress, autophagy produces metabolic substrates to meet the bioenergetic needs of the cell, thus preventing cell death (7). Therefore, it is necessary to evaluate the protective efficacy of an antioxidant from the perspective of autophagy. In auditory cells, oxidative stress induces autophagy through molecular crosstalk among p62, Keap1 and Nrf2 to provide protection against necrosis by ATP depletion (8). This suggests that autophagy may work together with the Keap1/Nrf2 pathway to resist oxidative stress.

Flavonoids are commonly found in medicinal plants, vegetables and fruits, and are known to significantly reduce the incidence of cardiovascular disease. Quercetin-3-O-α-L-rhamnopyranoside (QI; molecular weight, 448; Fig. 1A) is a natural polyphenol that belongs to the flavonoid family and is produced in the leaves of *Lindera aggregata* (Sims) Kosterm. QI has a wide range of pharmacological activities, including antioxidant (9), antiviral (10), antidepressant (11), diabetic resistant (12), liver protectant (13) and cardiovascular protectant activities (14). It has been reported that QI reduces the apoptosis of endothelial progenitor cells caused by oxidized low-density lipoprotein, and promotes autophagy via extracellular signal-regulated kinase activation (15). However, the underlying mechanism of the action of QI requires further investigation.

In the present study, the aim was to examine whether QI exerted a protective effect on human umbilical vein endothelial cells (HUVECs) and if it activated the Nrf2 pathway by inducing autophagy. The results revealed that the antioxidant effect of QI occurred at the gene level. *In vivo*, QI significantly improved the activity of superoxide dismutase (SOD) and glutathione (GSH), and decreased malondialdehyde (MDA) levels in the serum and heart tissue of aging rats. These results suggest that QI may be used in the early treatment of cardiovascular disease, or serve as a health supplement to alleviate oxidative stress.

Materials and methods

Reagents. Antibodies against light chain 3B (LC3B; cat. no. 3868), Caspase-9 (cat. no. 9502), Caspase-3 (cat. no. 9662), poly(ADP-ribose) polymerase (PARP; cat. no. 9532), autophagy related 5 (Atg5; cat. no. 12994), Atg13 (cat. no. 13468), Bach1 (cat. no. 4578) and β-actin (cat. no. 3700) were purchased from Cell Signaling Technology, Inc. (Beverly, MA, USA), while antibodies against Nrf2 (cat. no. R1312-8), heme oxygenase-1 (HO-1; cat. no. ET1604-45), and Histone H3 (cat. no. ET1601-14) were obtained from HuaBio (Hangzhou, Zhejiang, China). The secondary antibodies used in the present study included goat anti-rabbit horseradish peroxidase (HRP)-conjugated immunoglobulin (Ig)-G and goat anti-mouse HRP-conjugated IgG (cat. nos. BL003A and BL001A; Biosharp, Shanghai, China), as well as FITC goat anti-rabbit IgG (HA1004, HuaBio, Hangzhou, Zhejiang, China). Control (CTL), Nrf2 and HO-1 small interfering (si)-RNAs (cat. nos. sc-37007, sc-37030 and sc-35554, respectively) were purchased from Santa Cruz Biotechnology, Inc. (Dallas, TX, USA), while Lipofectamine® 2000 transfection reagent and dimethyl sulfoxide (DMSO) were purchased from Thermo Fisher Scientific, Inc. (Waltham, MA, USA). 3-Methyladenine (3-MA), chloroquine (CQ) and *N*-acetyl-L-cysteine (NAC) were purchased from Sigma-Aldrich (Merck KGaA, Darmstadt, Germany), H_2O_2 was obtained from Tianjin Yongda Chemical Reagent Co., Ltd. (Tianjin, China), while 3-(4,5-dimethylthiazol-2-yl)-2,5-diphenyl-2H-tetrazolium bromide (MTT) and Triton X-100 were from Solarbio Science & Technology Co., Ltd. (Beijing, China). The following kits were used in this study: ROS determination kit, total SOD assay kit (hydroxylamine method), MDA kit and reduced GSH assay kit, all purchased from Jiancheng Bioengineering Institute (Nanjing, China); BCA protein concentration determination kit and enhanced chemiluminescence (ECL) system, both from Beyotime Institute of Biotechnology (Shanghai, China); and Annexin V-FITC apoptosis detection kit, DNA Purification kit, and Nuclear and Cytoplasmic Protein Extraction kit, which were obtained from KeyGen Biotech Co., Ltd. (Nanjing, China).

QI preparation. Young leaves of *Lindera aggregate* (Sims) Kosterm. were collected from the Tiantaishan district (Zhejiang, China) and authenticated by Professor Jingkui Tian in Zhejiang University (Hangzhou, China), where the voucher specimens were stored and evaluated during our previous study (no. LA201301-08) (16). Separation, purification and structural analysis of QI were performed as described in a previous study (16). Briefly, dried plant material (10 kg) was extracted using 70% ethanol under reflux for 2 h, and the process was repeated three times. All the extracts were combined and concentrated under a vacuum. The combined extracts were diluted with H_2O and chromatographed over an AB-8 resin column, prior to eluting with NaOH (1 BV; pH 9.0), H_2O (3 BV) and 50% ethanol (3 BV). Subsequently, the 50% ethanol elution was concentrated and chromatographed on a reverse phase silica gel column (sample amount, 1 g; intermediates, 40 ml column volume; ethanol concentration, 14.25%; elution, 3 BV/h). Finally, an ethanol-water system was used for re-crystallization, and the solution was then set aside for 24 h at room temperature to obtain the QI.

Cells and culture conditions. Human umbilical vein endothelial cells (HUVECs) were obtained from the American Type Culture Collection (Manassas, VA, USA). Cells were cultured in Endothelial Cell Medium (ECM; ScienCell Research Laboratories, Inc., San Diego, CA, USA) supplemented with 5% fetal bovine serum (FBS) and 1% penicillin/streptomycin solution (100 IU/ml penicillin and 100 mg/ml streptomycin). The cells were maintained in a 37˚C humidified incubator with 5% CO_2.

MTT assay to determine cytotoxicity, cell viability and the effect of the autophagy inhibitor 3-MA. The cytotoxicity of QI was evaluated by an MTT assay. Briefly, cells were seeded in 96-well plates at $3x10^4$ cells/well in a final volume of 100 µl. After 16 h, fresh FBS-free medium with various concentrations of QI (0, 62.5, 125, 250 and 500 µM) was added to each well. Following 24 h of incubation, 20 µl MTT (5 mg/ml) per well was added, and the cells were incubated for a further 2 h. Subsequently, DMSO was used to dissolve the formazan

crystals, and a microplate reader was used to measure the optical density at 570 nm. Untreated cells were set to 100% viability in order to determine the cytotoxicity of QI.

The antioxidant properties of QI on cell viability were also assessed using MTT assay. Briefly, cells or transfected cells were treated with DMSO, H_2O_2 only or H_2O_2 (1,400 μM) and QI (62.5, 125, 250 and 500 μM) combined for 3 h. As described earlier, the medium was removed and replaced by 20 μl MTT (5 mg/ml). After 2 h, the supernatants were removed from the wells, and MTT dye was solubilized in DMSO at 200 μl/well. The absorbance at 570 nm was determined on a microplate reader.

HUVECs were seeded into 96-well plates at $3x10^4$ cells/well in a final volume of 100 μl. When completely adherent, cells were treated with 25 μM 3-MA (an autophagy inhibitor) for 1 h at 37˚C, followed by QI treatment as aforementioned. Following 3 h, the medium was replaced with fresh FBS-free ECM, and 20 μl MTT (5 mg/ml) was added to each well for a further 2 h incubation. The crystals were then dissolved in DMSO and the optical density at 570 nm was detected using a microplate reader following high-speed vibration for 3 min. The cell viability was calculated by considering untreated cells as 100% viable.

Plasmid transfection and observation of apoptosis morphology. Cells were transfected with plasmids encoding red fluorescent protein (RFP; Addgene, Inc., Cambridge, MA, USA) using the VigeneFection (VGF) plasmid transfection reagent (Vigene Biosciences, Inc., Rockville, MD, USA), according to the manufacturer's protocol. Briefly, cells were treated with 0.5 μg plasmid DNA and 2 μl VGF in each well of a 24-well plate. Then HUVECs were seeded in confocal dishes following 24 h of stable transfection. The expression of RFP in HUVECs was confirmed by fluorescence detection. When 80-90% confluence was reached, treatments were initiated. Confocal images were obtained with an Olympus FV1000 confocal microscope (Olympus Corp., Tokyo, Japan).

Transient transfection with siRNA. Cells were seeded in 6-well plates at $5x10^5$ cells/well and then transfected with the CTL siRNA (17), Nrf2 siRNA (18) or HO-1 siRNA (19) using Lipofectamine 2000™. Briefly, 3 μg of siRNA was added to each well with 6 μl Lipofectamine 2000™. Treatments were initiated following 24 h transfection. The expression of the Nrf2 and HO-1 proteins was confirmed by western blot analysis.

SOD, GSH, and MDA assay in HUVECs. HUVECs were cultured at a density of $2x10^5$ per well in 6-well plates and cultured overnight and then treated with H_2O_2 (1,400 μM) and QI (62.5, 125, 250 and 500 μM) for 3 h. Then cells were collected and assay kits (Jiancheng Bioengineering Institute) were used to measure the activity of MDA, GSH and SOD.

Cell apoptosis analysis. The role of QI in protecting HUVECs from H_2O_2-induced apoptosis was assessed by flow cytometry using an Annexin V-FITC apoptosis detection kit. Briefly, cells were harvested by non-enzymatic cell dissociation and centrifuged (500 x g for 5 min at room temperature) to remove the medium. The cells were then washed twice with phosphate-buffered saline (PBS) prior to re-suspending in 500 μl binding buffer. Next, the cells were stained with 5 μl Annexin V-FITC and 5 μl propidium iodide (PI). After 15-min incubation without exposure to light, the Annexin V and PI emissions were detected in the FL1-H and FL2-H channels, respectively, with an excitation wavelength of 488 nm and emission wavelength of 530 nm on a FACS-Vantage flow cytometer (Cytomics FC 500; Beckman Coulter, Inc., Brea, CA, USA).

DNA ladder assay. HUVECs were seeded in 6-well plates at a concentration of $7.0x10^5$ cells/well. At 16 h after planting, the cells were treated with H_2O_2 with or without QI. Following the treatment, DNA was isolated with a DNA Purification kit and electrophoretically analyzed on 1.5% agarose gel.

ROS assay. Cells were seeded into 6-well plates at $5x10^5$ cells/well and treated with H_2O_2 and QI at a range of concentrations for 3 h. The medium was removed and replaced with 1 ml PBS containing 1 μM CM-H_2DCFDA (Jiancheng Bioengineering Institute), and cells were then incubated in a 5% CO_2 incubator at 37˚C for 30 min in the dark. Next, the cells were collected in 15 ml centrifuge tubes. Subsequent to washing with PBS three times, the ROS level for each treatment group was determined using a flow cytometer (Cytomics FC 500) and analyzed using FlowJo software (version 7.6; FlowJo LLC, Ashland, OR, USA).

Nuclear transfer of Nrf2. Cells treated with QI and H_2O_2, or pretreated with 3-MA (25 μM) were washed with cold PBS and fixed with methanol (pre-chilled at -20˚C) for 5 min at room temperature. Next, cells were permeabilized with 0.5% Triton X-100 in PBS for 10 min and then blocked with 1% bovine serum albumin (BSA) in PBS for 30 min. Following washing with PBS, the cells were incubated overnight with an anti-Nrf2 antibody in 1% BSA at 4˚C, followed by incubation with FITC goat anti-rabbit IgG in 1% BSA for 2 h at room temperature. Nuclei were stained with DAPI in Vectashield mounting medium (Vector Laboratories, Inc., Burlingame, CA, USA). Confocal images were obtained using the 63x oil immersion lens on a confocal microscope (LSM 780; Carl Zeiss AG, Oberkochen, Germany).

Western blot analysis. Drug-treated cells were collected by scraping, followed by centrifugation (500 x g for 5 min at 4˚C). Nuclear and cytoplasmic proteins were extracted according to the protocol of the Nuclear and Cytoplasmic Protein Extraction kit. The extraction of total protein was performed as follows: Cells were washed once with PBS and then lysed in a lysis buffer consisting of 1% sodium dodecyl sulfate (SDS), 10 mM ethylene diamine tetra acetic acid (EDTA) and 50 mM Tris-HCl (pH 8.1) in the presence of a 1% protease inhibitor mixture (Sigma-Aldrich; Merck KGaA). Lysates were sonicated (15 sec) to shear genomic DNA and then centrifuged at 13,000 x g for 10 min at 4˚C. The protein concentrations in the supernatants were determined using the Micro BCA Protein Assay kit. Equal protein amounts were resolved on an SDS-polyacrylamide gel and transferred to a polyvinylidene fluoride membrane (Bio-Rad Laboratories, Inc., Hercules, CA, USA). The membrane was then blocked with 5% non-fat milk in Tris-buffered saline containing 0.1% Tween-20 (TBST)

for 30 min at room temperature, and then incubated with the LC3B (1:1,000), Capase-9 (1:500), Caspase-3 (1:500), PARP (1:1,000), Atg13 (1:500), Atg5 (1:500), Nrf2 (1:500), HO-1 (1:500), Bach-1 (1:500), Histone H3 (1:1,000) and β-Actin (1:1,000) antibodies in TBST at 4˚C overnight. The membrane was then washed three times with TBST for a total of 30 min, followed by incubation with goat secondary antibodies against rabbit or mouse IgG conjugated to HRP (1:5,000 dilution) for 2 h at room temperature. Subsequent to washing three times with TBST for a total of 30 min, ECL was used to develop the images and the immunoblots.

Detection of autophagic flux and the effect of ROS on autophagy. HUVECs were seeded into 6-well-plates, and then separately treated with CQ (10 μM) or QI (250 μM), or co-treated with CQ and QI for 3 h. Cells were subsequently lysed to determine LC3B and β-actin levels by western blot analysis. Furthermore, cells that were separately treated with QI (0, 62.5, 125 and 250 μM) and NAC (5 mM) only or NAC pretreatment for 1 h with QI (62.5, 125 and 250 μM) were also lysed to determine LC3B and β-actin levels by western blot analysis.

Fluorescent quantitative polymerase chain reaction (qPCR). Briefly, HUVECs were seeded into 96-well plates at $3x10^4$ cells/well. Following treatment of cells with QI, the medium was removed and cells were washed with 50 μl cold PBS. For the extraction of cellular RNAs, the ExCellenCT Lysis kit (Applied Biological Materials, Inc., Richmond, BC, Canada) was used according to the manufacturer's protocol. A total of 1 μl protease and 50 μl lysis solution were added to each well, mixed and incubated for 10 min in an incubator. To end the reaction, 1 μl protease inhibitor and 5 μl stop solution were added and incubated for 20 min at room temperature. Next, the RNA concentration was measured with a microplate reader. Reverse transcription was conducted in an RNase-free environment using 5X All-In-One RT MasterMix (Applied Biological Materials, Inc.) according to the manufacturer's protocol. The reverse transcription system contained 2 μl 5X All-In-One RT MasterMix, 13 μl nuclease-free water and 5 μl total RNA (2 μg). The reverse transcription conditions were as follows: 25˚C for 15 min, 42˚C for 30 min, 85˚C for 5 min, and then held at 4˚C. Subsequent to reverse transcription, EvaGreen 2X qPCR MasterMix (Applied Biological Materials, Inc.) was applied in a reaction system containing 0.3 μl forward primer (10 μM), 0.3 μl reverse primer (10 μM), 0.6 μl cDNA (10 ng/μl), 5 μl EvaGreen and 3.8 μl H_2O. The qPCR reaction conditions (25˚C for 15 min, 42˚C for 30 min, 85˚C for 5 min, and then held at 4˚C) were similar to those of reverse transcription. The primers used in the present study were as follows: β-actin forward, 5'-CGGGAAATCGTGCGTGACAT-3', and reverse, 5'-GAACTTTGGGGGATGCTCGC-3'; Nrf2 forward, 5'-GATTCTGACTCCGGCATTTC-3', and reverse, 5'-TCCCCAGAAGAATGTACTGG-3'; and HO-1 forward, 5'-GCCCTGCCCTTCAGCAT-3', and reverse, 5'-CTGCATTTGAGGCTGAGCC-3'. The relative quantification $2^{-\Delta\Delta Cq}$ method (20) was used to evaluate quantitative variation between treatments.

In vivo study. In the present study, 50 specific-pathogen-free female rats of the Sprague-Dawley strain (>18 weeks; 500-550 g; JOINN Laboratories, Suzhou, China) were housed in groups under a 12-h light/dark cycle, at a constant temperature of 24˚C and humidity of 40%; all animals were provided with sterilized food and water *ad libitum*. Following 7 days of acclimatization, the animals were randomly distributed into five groups, each containing 10 animals of similar average body weight. Animals in the five groups received the following treatments: i) Vehicle (20% polyethylene glycol 2000 and 10% polyethylene glycol 400 in saline); ii) 4.0 mg/kg breviscapine, a Chinese medicine used to treat cardiovascular and cerebrovascular diseases (21), serving as a positive control; iii) QI at a dose of 4.0 mg/kg; iv) QI at a dose of 8.0 mg/kg; and v) QI at a dose of 16.0 mg/kg. All treatments were administered by tail vein injection once daily for 2 weeks. All experimental procedures using live animals were conducted in accordance with protocols approved by the Ethics Review Committee for the Use of Animal Subjects of Zhejiang University (Zhejiang, China).

Preparation of homogenates. Animals underwent a 12-h fast from food prior to sacrifice, and then hearts were collected. Tissue homogenates were prepared by grinding 0.1 g of the tissue in 1 ml saline. Following centrifugation at 1,500 x g for 15 min at 4˚C, the supernatant was removed and kept at -20˚C until further use.

Preparation of sera and evaluation of biochemical parameters. Blood was collected by orbital puncture from the rats, following anesthesia by ethyl ether. The blood samples were then allowed to settle for 30 min prior to centrifugation at 2,500 x g for 10 min at 4˚C. Sera and heart tissue homogenates were used for detecting biochemical parameters associated with oxidative stress, including SOD, GSH and MDA, according to the protocols of the corresponding kits.

Statistical analysis. Data are presented as the mean ± standard deviation. One-way analysis of variance and least significant difference tests were used for statistical analysis in all experiments. Differences were considered to be statistically significant at $P<0.05$. Statistical analyses were performed using the SPSS statistical software (version 17.0; SPSS, Inc., Chicago, IL, USA).

Results

QI promotes the growth of HUVECs. The MTT cell proliferation assay was used to assess QI toxicity. QI promoted the growth of HUVECs at all the investigated concentrations (62.5-500 μM), and significantly accelerated cell proliferation at the concentrations of 62.5 and 125 μM (Fig. 1B). Treatment with 62.5, 125, 250 and 500 μM QI for 24 h increased cell viability by 5.75, 3.14, 1.44 and 0.49%, respectively, compared to the control (Fig. 1B). These findings suggest that, at concentrations ranging between 62.5 and 500 μM, QI does not damage HUVECs.

QI protects HUVECs from damage induced by H_2O_2. The study next investigated the effect of QI on the growth of HUVECs following H_2O_2-induced oxidative damage. The HUVECs ultimately demonstrated apoptosis-like changes in their

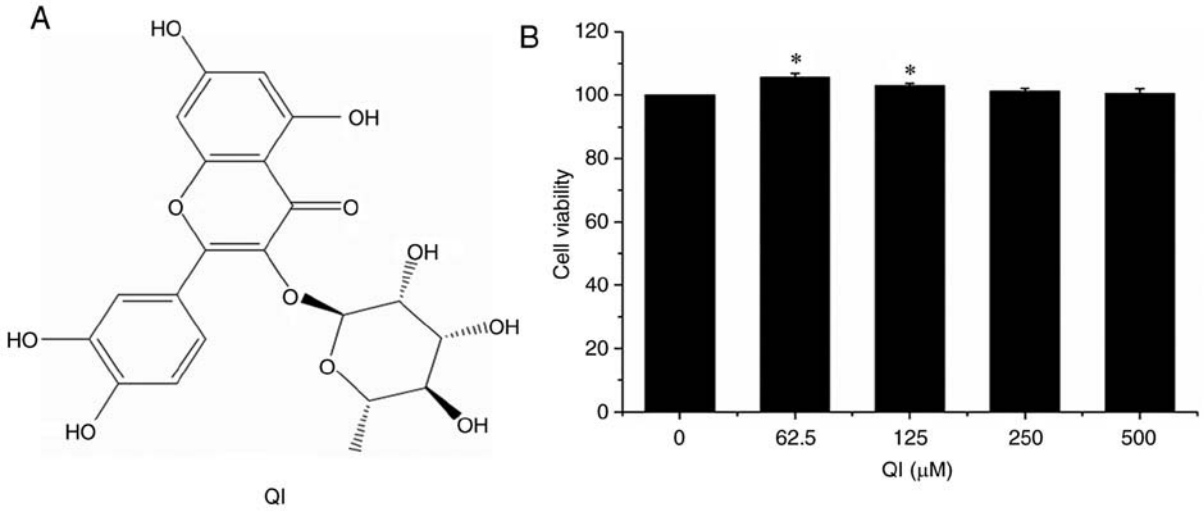

Figure 1. QI treatment results in moderate promotion of human umbilical vein endothelial cell growth. (A) Chemical structure of QI. (B) Cell viability assessment following QI treatment for 24 h in fetal bovine serum-free medium. All assays were performed in triplicate, and data are expressed as the mean ± standard deviation (treated vs. control cell viability). *P<0.05 vs. the control. QI, Quercetin-3-O-α-L-rhamnopyranoside.

morphology, including plasma rounding and cell shrinkage, as a result of oxidative injury in the H_2O_2-treated group (Fig. 2A). By contrast, fewer apoptotic-like cells were observed in the cell groups co-treated with various concentrations of QI and H_2O_2 (Fig. 2B). Co-treatment with 62.5, 125, 250 or 500 μM QI resulted in significant dose-dependent protection against cell death induced by 1,400 μM H_2O_2 (Fig. 2C).

QI reduces H_2O_2-induced increases in MDA level, and improves intracellular SOD and GSH activities in HUVECs. Incubation of HUVECs with H_2O_2 for 3 h significantly increased MDA levels, and decreased SOD and GSH activities as compared with those in the control group. However, co-treatment of HUVECs with QI significantly reduced the H_2O_2-induced MDA levels and restored the SOD and GSH activities compared with the group treated with H_2O_2 alone, in a concentration-dependent manner (Fig. 2D-F). In comparison with the H_2O_2-treated group, cells treated with 62.5, 125, 250 and 500 μM QI displayed increased SOD levels by 89.10, 138.61, 181.19 and 198.02%, respectively. A similar improvement was observed in GSH activity following QI treatment in HUVECs, with a significant increase detected (Fig. 2E). Compared with the H_2O_2-only group, the cell groups treated with 62.5, 125, 250 and 500 μM QI displayed a markedly higher content of GSH by 13.89, 43.18, 76.26 and 102.02%, respectively. By contrast, MDA was reduced by 29.31, 43.10, 51.72 and 67.24% in the 62.5, 125, 250 and 500 μM QI-treated cells, respectively, as compared with the H_2O_2 treatment alone.

QI inhibits H_2O_2-induced apoptosis in HUVECs. Staining with Annexin V-FITC/PI and flow cytometry were performed to identify the apoptotic cells. The results revealed that cells exposed to H_2O_2 alone exhibited a higher apoptotic rate (46.7±3.3%) as compared with the control cells (1.3±0.1%). A two-dimensional diagram also revealed that QI treatment at concentrations of 62.5, 125, 250 and 500 μM decreased the proportion of apoptotic cells to 30.3±1.8, 26.9±1.7, 19.3±1.4 and 18.4±0.8%, respectively, as compared with that observed in cells that suffered H_2O_2 injury (Fig. 3A and B).

The present study further investigated whether H_2O_2 caused DNA fragmentation, which is another hallmark of apoptosis, in HUVECs. Agarose gel electrophoresis revealed that HUVECs treated with H_2O_2 exhibited DNA fragmentation, as indicated by the typical DNA laddering pattern, whereas QI-treated cells demonstrated significantly reduced DNA laddering (Fig. 3C). Additionally, treatment with QI resulted in a dose-dependent decrease in cleaved Caspase-3 and PARP levels, as well as activation of Caspase-9, compared with the H_2O_2 treatment alone (Fig. 3D). Collectively, these results indicate that QI protects against cell death by inhibiting H_2O_2-induced apoptosis.

QI inhibits the production of ROS triggered by H_2O_2. Oxidative stress inhibition was further corroborated by the fact that QI mediated decreases in H_2O_2-induced ROS production in the HUVECs. The rate of ROS-positive cells was decreased from 94.2±1.1% in the 62.5 μM QI-treated group to 73.2±2.7% in the 500 μM QI-treated group, as compared with the ROS rate of 97.1±2.3% in the H_2O_2 treatment alone group (Fig. 4A and B). These results indicate that QI provides resistance to ROS in a dose-dependent manner.

QI protects HUVECs from H_2O_2-induced cytotoxicity through activation of the Keap1/Nrf2 pathway and inhibition of Bach1. In light of the aforementioned findings, the pathways involved in QI-mediated protection against oxidative stress were examined in HUVECs by immunofluorescence and western blot assays. Nrf2 is essential for cytoprotection against oxidative stress (22). The present study revealed that nuclear Nrf2 levels were increased subsequent to QI treatment, as indicated by both the immunofluorescence and western blot assay results; Histone H3 was used as a nuclear internal reference (Fig. 5A-C). Furthermore, Bach1 nuclear expression was decreased in QI-treated cells, but was increased in the cytoplasm, indicating that QI promoted the transfer of Bach1

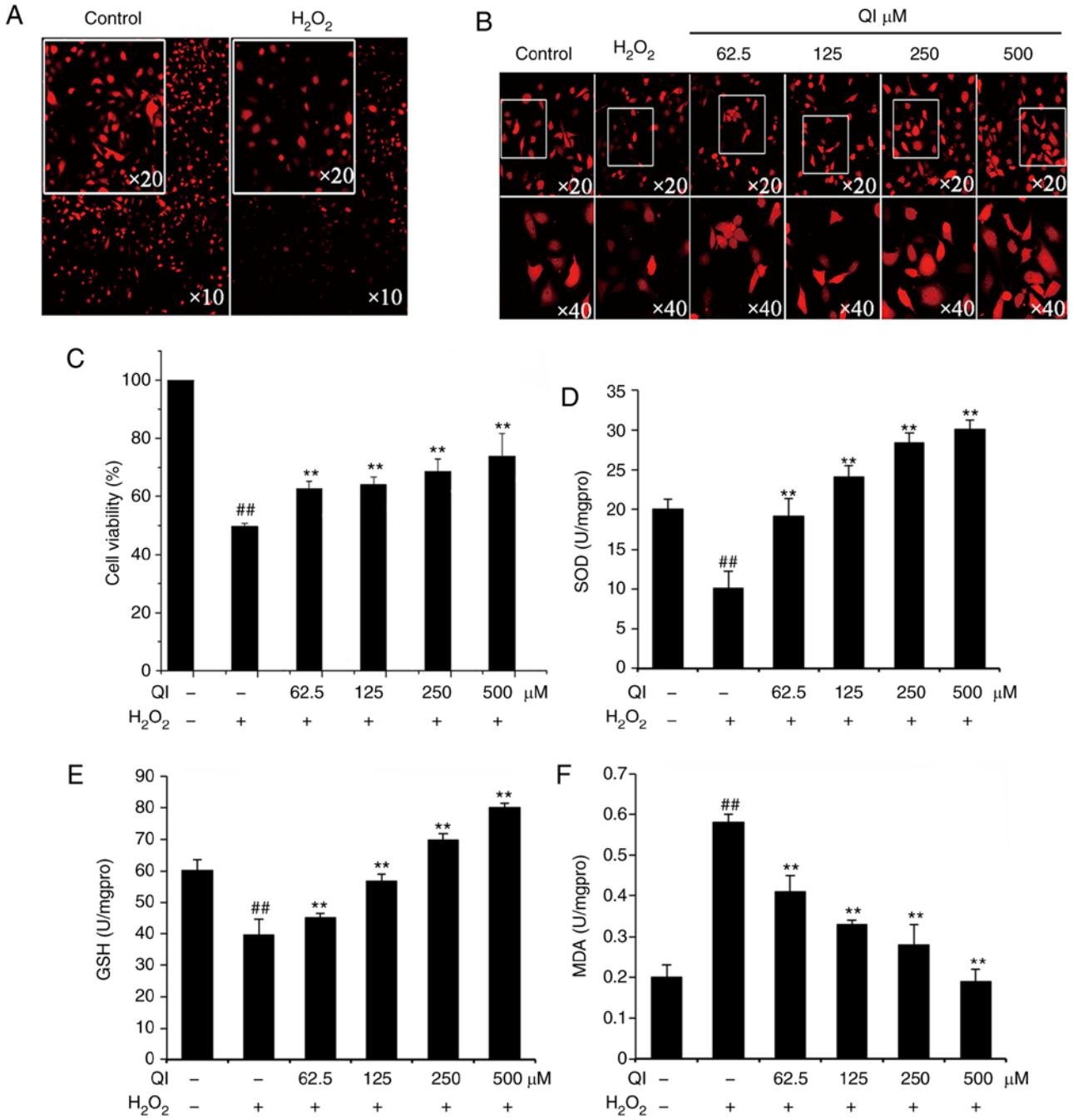

Figure 2. QI protects HUVECs from H_2O_2-induced apoptosis by increasing SOD activity and GSH content. Confocal images examining the morphology of cells treated with (A) H_2O_2 alone and (B) H_2O_2 in combination with QI, demonstrating the protective effect of QI against H_2O_2-induced oxidative stress injury in red fluorescent protein-stained HUVECs (magnification, x10, x20 or x40). (C) Effect of QI on the viability of HUVECs following H_2O_2-induced damage was measured by an MTT assay. Data are expressed as the percentage of viable cells (treated vs. control cells). (D) SOD and (E) GSH intracellular activities of HUVECs were improved by QI treatment, while (F) MDA activity was reduced. Cells were treated with H_2O_2 and QI for 3 h at 37˚C, and then the SOD, GSH and MDA activities were determined by the corresponding assay kits. All assays were performed in triplicate, and data are expressed as the mean ± standard deviation. $^{\#\#}$P<0.01 vs. control; **P<0.01 vs. H_2O_2 treatment. QI, Quercetin-3-O-α-L-rhamnopyranoside; HUVECs, human umbilical vein endothelial cells; SOD, superoxide dismutase; GSH, glutathione; MDA, malondialdehyde.

from the nucleus to the cytoplasm, thus releasing its inhibitory effect on Nrf2 (Fig. 5C). The expression of HO-1 protein, which acts downstream of Nrf2, was also increased following QI treatment (Fig. 5D), suggesting that the antioxidant effect of QI was regulated by the Nrf2 antioxidant pathway.

QI upregulates the expression levels of the Nrf2 and HO-1 genes. qPCR was used to further investigate the antioxidative mechanism of QI *in vitro*. The data demonstrated that the expression levels of Nrf2 and HO-1 genes increased following QI treatment (Fig. 6A). Taken together, these results revealed that QI affects both the protein levels of Nrf2 and HO-1, as well as their transcriptional levels.

Nrf2 inhibition suppresses QI-induced antioxidant expression and cytoprotection. As mentioned earlier, nuclear localization

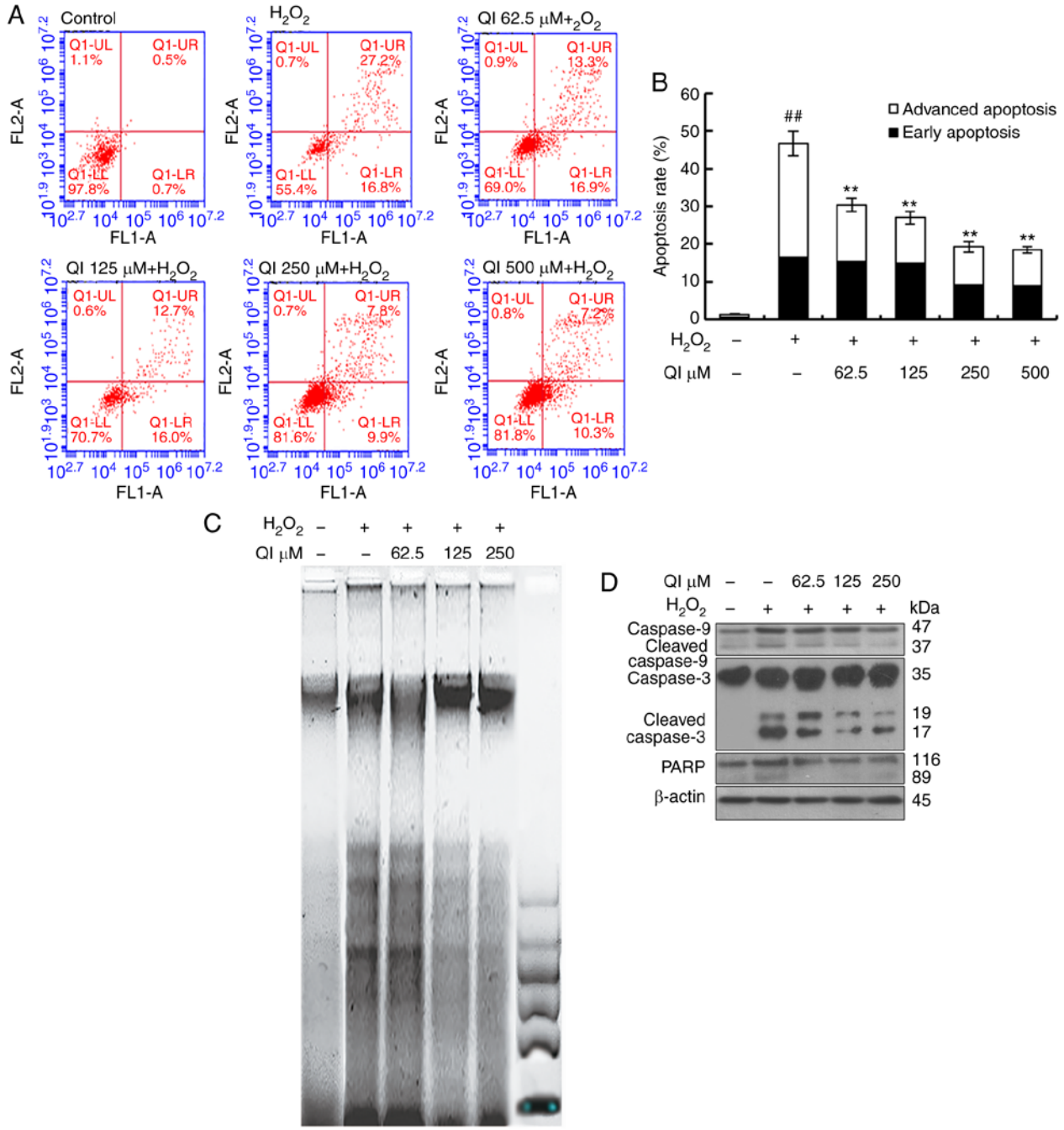

Figure 3. Inhibitory effect of QI on cell apoptosis that was induced by H_2O_2. (A) Representative dot-plots of living, early apoptotic and late apoptotic/necrotic cells, as determined by flow cytometry with Annexin V and PI double staining. HUVECs were incubated in drug-free medium, or medium containing H_2O_2 and QI for 3 h. The horizontal axis represents the Annexin V intensity, and the vertical axis represents the PI staining. (B) Apoptosis rate analysis. All assays were performed in triplicate, and data are expressed as the mean ± standard deviation. $^{\#\#}$P<0.01 vs. control; **P<0.01 vs. H_2O_2 treatment. (C) QI inhibited H_2O_2-induced DNA damage in HUVECs. Fragmented DNA was extracted and analyzed on 1.5% agarose electrophoresis gels. (D) Western blot analysis of Caspase-9, cleaved Caspase-9, Caspase-3, cleaved Caspase-3 and PARP protein expression levels in HUVECs following H_2O_2 treatment with or without QI. HUVECs, human umbilical vein endothelial cells; QI, Quercetin-3-O-α-L-rhamnopyranoside; PARP, poly(ADP-ribose) polymerase.

of Nrf2 was found to be increased, while Nrf2 gene expression was upregulated by QI under oxidative stress conditions (Figs. 5 and 6A). Therefore, the study further examined whether reducing Nrf2 expression using siRNA transfection affects antioxidants. Nrf2 is known to activate the transcription of numerous cytoprotective enzymes, such as HO-1. The current study results revealed that Nrf2 siRNA transfection suppressed the effect of QI on increased HO-1 expression under oxidative stress conditions (Fig. 6B).

Next, the study examined whether Nrf2 siRNA or HO-1 siRNA were able to suppress the QI-induced cytoprotection in HUVECs by assessing the cell viability using an MTT assay following siRNA transfection. QI significantly reduced the H_2O_2-induced cytotoxicity of HUVECs transfected with CTL siRNA, with a cell viability of 55.1% observed in the H_2O_2 group and 75.2% in the H_2O_2+QI group (P<0.05; Fig. 6C). By contrast, QI treatment did not markedly reduce the H_2O_2-induced cytotoxicity of HUVECs transfected with Nrf2

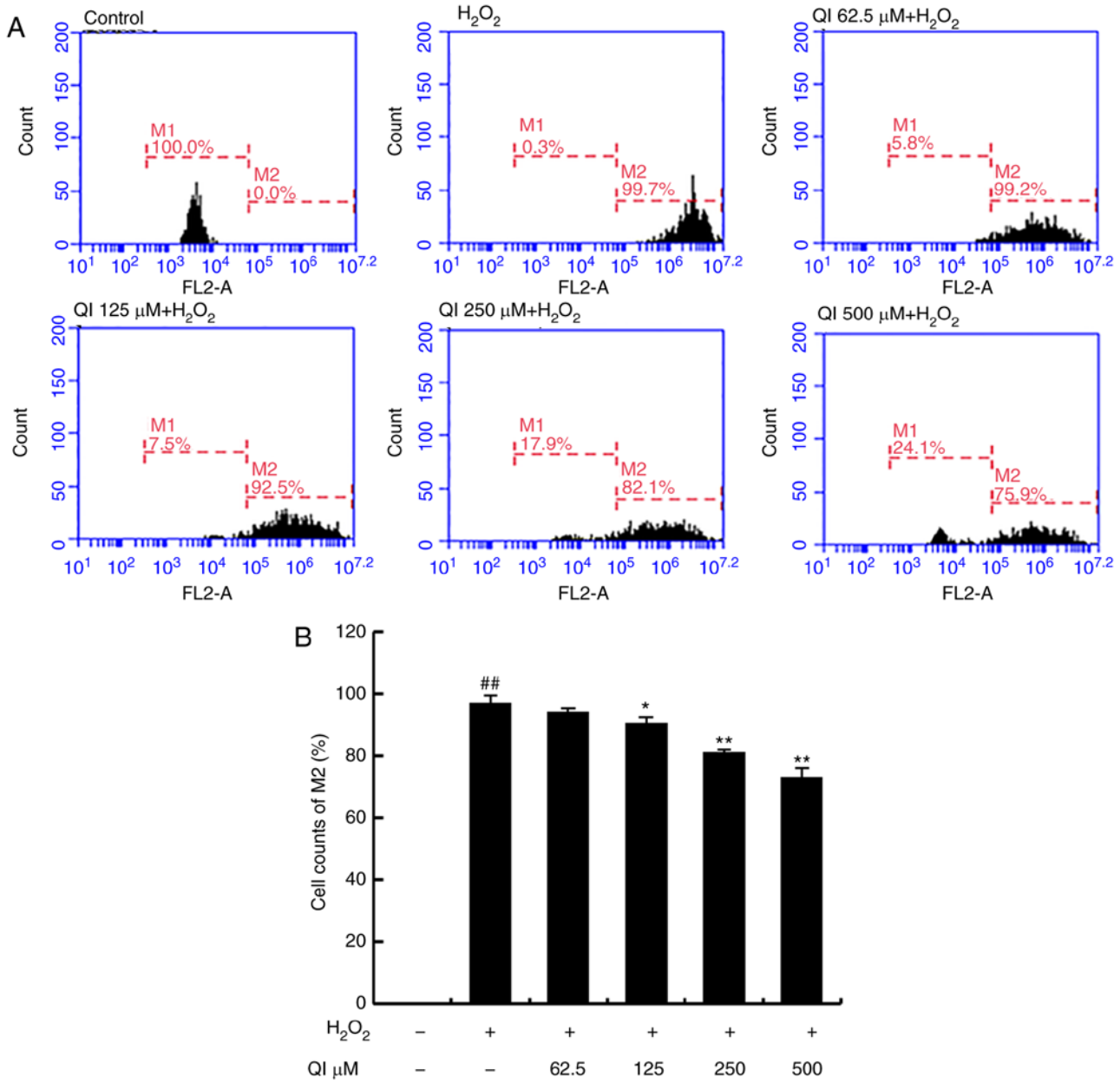

Figure 4. QI inhibits ROS production in human umbilical vein endothelial cells induced by H_2O_2. (A) ROS level of each QI concentration used, determined using a flow cytometer (Cytomics FC 500) and analyzed with FlowJo version 7.6 software, following treatment with QI and H_2O_2. M1 represents the negative signal, while M2 is the positive signal responding to ROS production. (B) Cell counts of M2 analysis. All assays were performed in triplicate, and data represent the mean ± standard deviation. $^{\#\#}$P<0.01 vs. control; *P<0.05 and **P<0.01 vs. H_2O_2 treatment. QI, Quercetin-3-O-α-L-rhamnopyranoside; ROS, reactive oxygen species.

siRNA (H_2O_2, 53.2%; H_2O_2+QI, 58.3%; P>0.05). However, in cells transfected with HO-1 siRNA, QI was able to reduce the H_2O_2-induced cytotoxicity, with a cell viability of 50.3 and 70.2% in the H_2O_2 and H_2O_2+QI groups, respectively (P<0.05; Fig. 6C). Fig. 6D presents the blots confirming that the transfection of Nrf2 siRNA and HO-1 siRNA resulted in successful knockdown. These results suggest that QI-induced Nrf2 nuclear transcription is critical for cytoprotection against oxidative stress.

QI promotes Nrf2 transcription and inhibits HUVEC damage by inducing autophagy. Autophagy detection was also performed in the present study. The expression levels of Atg5, Atg13 and the autophagic marker LC3B-II were increased following QI treatment (Fig. 7A and B). When combined with autophagy flux detection, treatment with both QI and CQ resulted in an evident improvement in LC3B-II levels as compared with that observed in cells with QI or CQ treatment alone (Fig. 7C), suggesting that QI promotes autophagy. To further assess whether ROS or QI induced autophagy, the ROS inhibitor NAC was used. The results found that addition of NAC had no effect on the QI-induced increase of LC3B-II levels (Fig. 7D), further demonstrating that QI can induce autophagy. Notably, the transfer of Nrf2 from the cytoplasm to the nucleus was inhibited by 3-MA, an autophagy inhibitor (Fig. 7E). To further test the hypothesis that autophagy is involved, the cell viability was measured following 3-MA pre-treatment. It was observed that the protective effect of QI

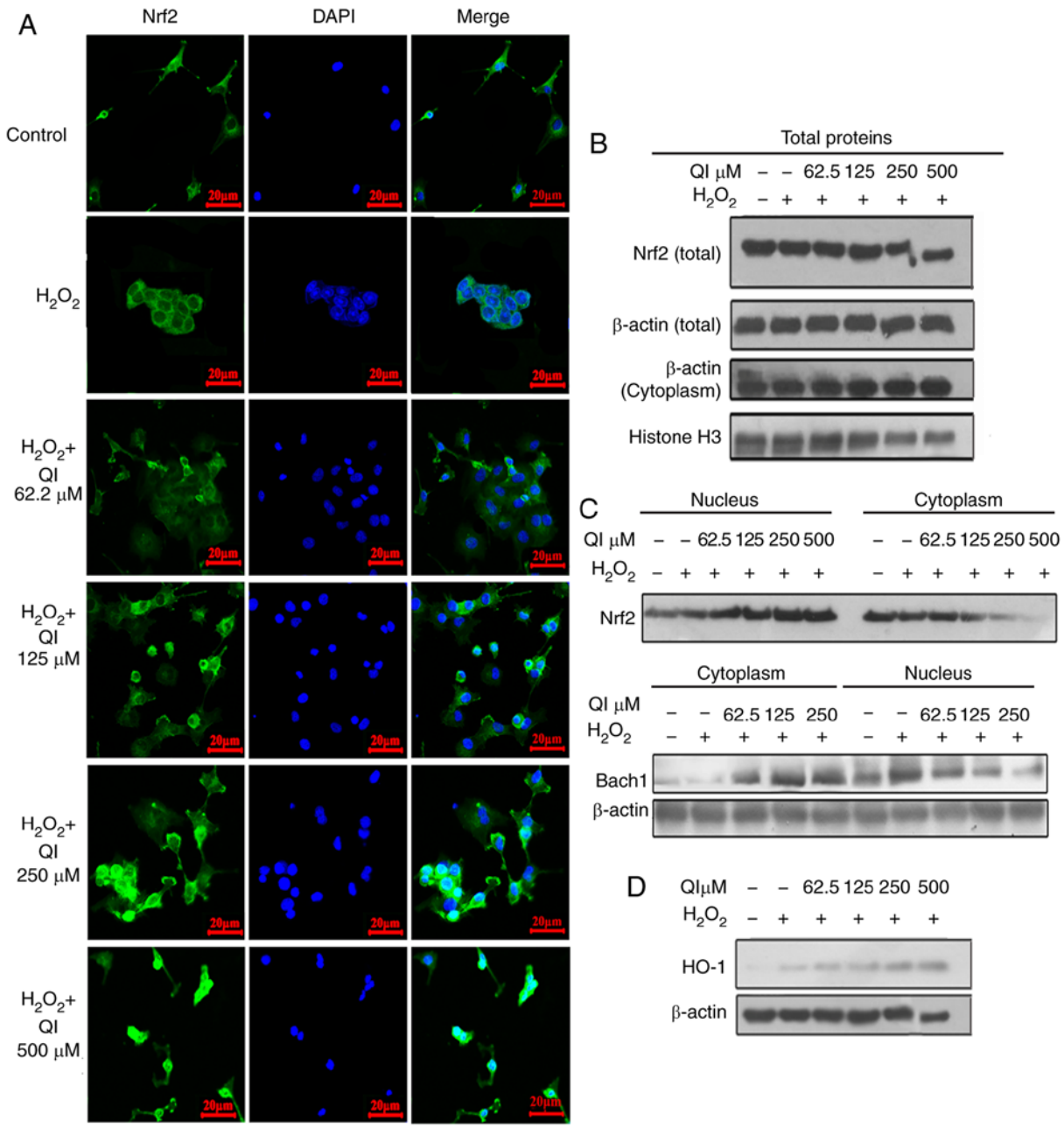

Figure 5. QI promotes Nrf2 nuclear transfer, increased the expression of the antioxidative protein HO-1 and inhibits Bach1 competition. (A) Immunohistochemical analysis of Nrf2 in human umbilical vein endothelial cells (blue, DAPI; green, Nrf2). Confocal images were obtained using the 63X oil immersion lens of a confocal microscope (scale bar, 20 μm). Western blot analysis results of (B) Nrf2 and Histone H3 total proteins, (C) Nrf2 and Bach1 protein levels in the nucleus and cytoplasm, and (D) HO-1 levels (an Nrf2 downstream protein). QI, Quercetin-3-O-α-L-rhamnopyranoside; Nrf2, nuclear factor erythroid 2-related factor 2; Bach1, BTB and CNC homolog 1; HO-1, heme oxygenase-1.

was diminished by the addition of 3-MA (Fig. 7F), indicating that QI serves its antioxidant role in HUVECs by inducing autophagy.

QI improves the activities of SOD and GSH, and decreases the content of MDA in the serum and heart tissue of rats. Next, rats were used to assess the antioxidant ability of QI *in vivo* (Fig. 8A). Our preliminary experimental results demonstrated that QI has no toxic or side effects on rats when administered at a dose of 0-100 mg/kg once daily for 2 weeks by tail vein injection (data not shown). In addition, the pre-experimental SOD vitality test results revealed that the lowest effective dose was 4 mg/kg (data not shown); therefore, the concentrations of 4, 8 and 16 mg/kg were selected for subsequent experiments. QI treatment displayed a dose-dependent reduction in MDA levels and increase in SOD activity. This effect reached a maximum level at the highest tested dosage (16 mg/kg) in the serum and heart tissue of rats (Fig. 8B and C). In the serum, QI at doses of 4, 8 and 16 mg/kg significantly enhanced GSH content, whereas only the 16 mg/kg dose was able to increase the GSH content in the heart tissue. These results indicate that QI achieves an antioxidant capacity in aging rats primarily through improving SOD, scavenging MDA and moderately increasing GSH.

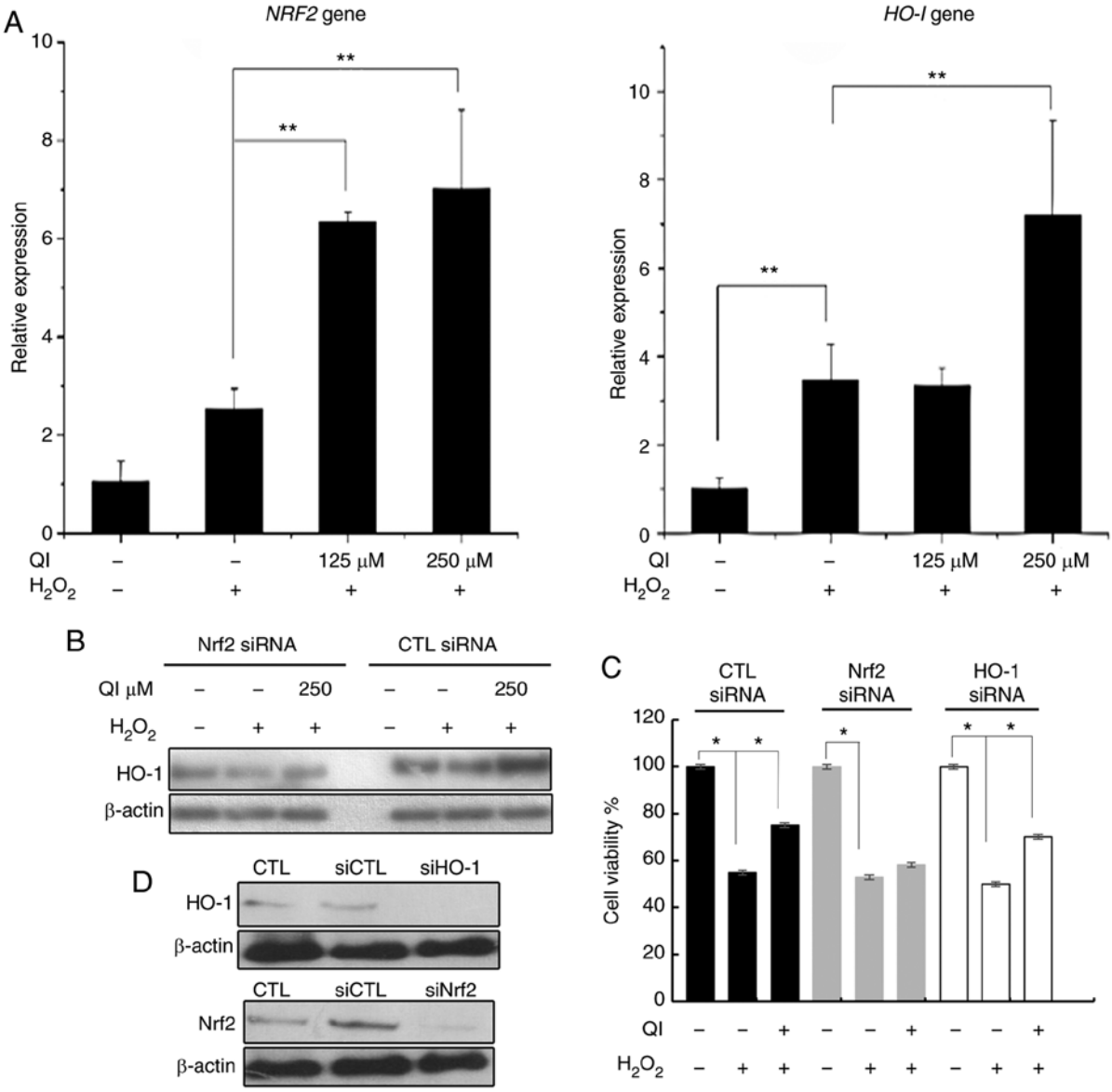

Figure 6. QI upregulates the expression of antioxidant genes Nrf2 and HO-1, while knockdown of Nrf2 by siRNA transfection suppresses the QI-induced antioxidant effect in HUVECs. (A) Quantitative polymerase chain reaction analysis of Nrf2 and HO-1 gene levels. (B) Western blot analysis of HO-1 protein expression in cells transfected with CTL and Nrf2 siRNA, followed by QI and H_2O_2 treatment. (C) Effect of QI on the viability of HUVECs with H_2O_2-induced damage was measured by an MTT assay following CTL, Nrf2 or HO-1 siRNA transfection (expressed as the percentage of viable cells; treated vs. control cells). (D) Western blot analysis was also performed to confirm that Nrf2 and HO-1 siRNA transfection resulted in successful knockdown. All assays were performed in triplicate, and data represent the mean ± standard deviation. *P<0.05 and **P<0.01, as indicated. QI, Quercetin-3-O-α-L-rhamnopyranoside; HUVECs, human umbilical vein endothelial cells; Nrf2, nuclear factor erythroid 2-related factor 2; HO-1, heme oxygenase-1; CTL, control; siRNA, small interfering RNA.

Discussion

Endothelial dysfunction has been implicated in the initiation and propagation of vascular diseases, including atherosclerosis, hypertension, cardiac hypertrophy and congestive heart failure. The oxidative stress induced by ROS, such as superoxide, H_2O_2 and peroxynitrite, is a key cause of endothelial cell dysfunction (23). The main chemical constituents in the leaves of *Lindera aggregata* (Sims) Kosterm. are flavonoids, which are known to have a favorable effect on the prevention and treatment of cardiovascular disease. In the present study, the antioxidant activity of QI derived from the leaves of *Lindera aggregata* (Sims) Kosterm. was investigated *in vitro* and *in vivo*. The results revealed that in QI treatment, autophagy serves an important role in regulating the Nrf2 pathway to protect HUVECs from damage caused by oxidative stress.

Oxidative metabolites are involved in the functional inactivation of endothelial cells by increasing cell permeability and as potent inducers of endothelial cell death. The MDA level reflects the extent of cell damage induced by oxidative stress (24). An oxidative stress model was established in the present study, according to the results of preliminary experiments, which identified that a concentration of 1,400 μM H_2O_2 resulted in a cell viability of ~50%. The antioxidant enzyme SOD and reducing compound GSH are considered to augment the antioxidant defenses in endothelial cells. SOD scavenges superoxide radicals by converting them to hydrogen peroxide,

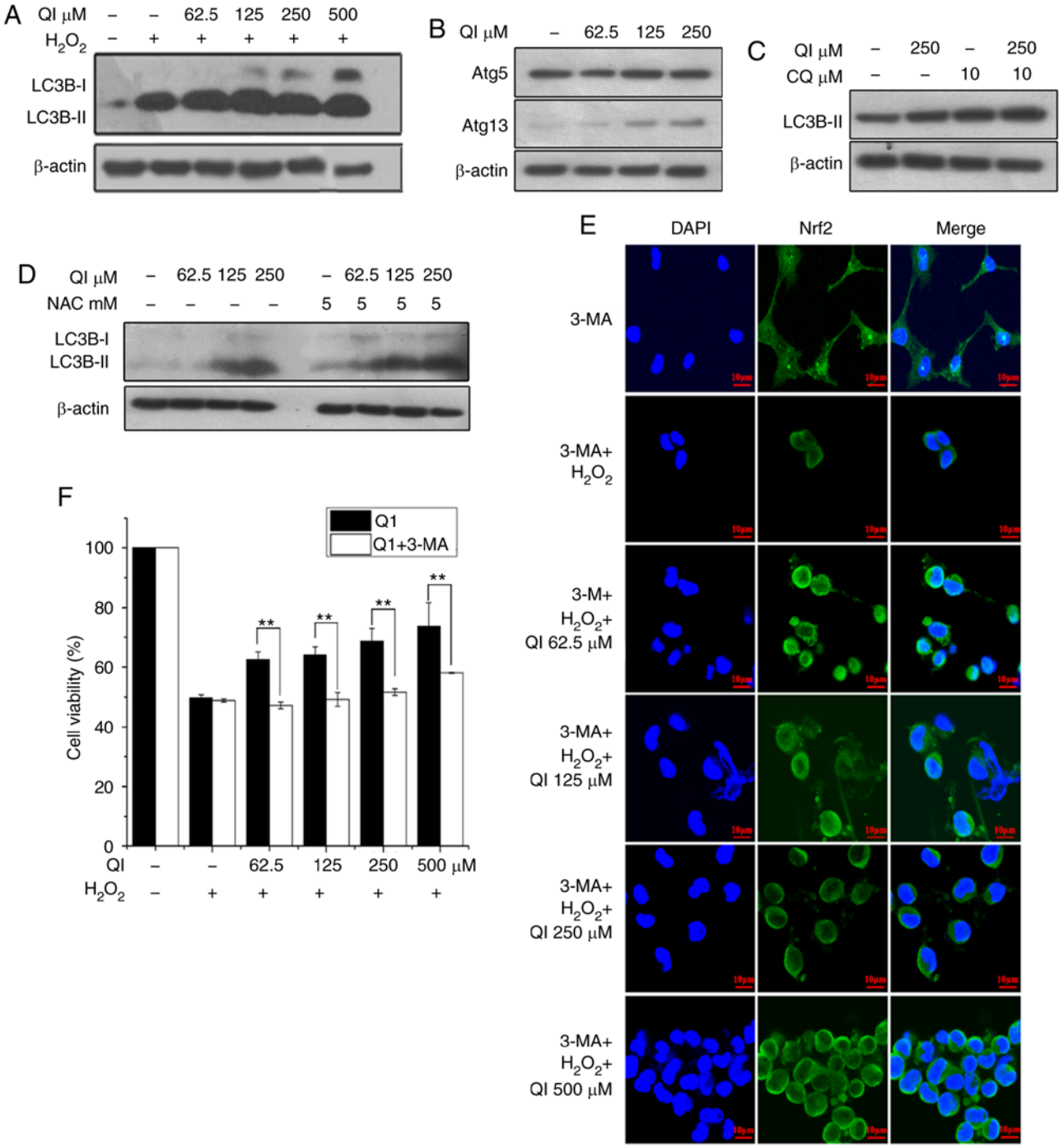

Figure 7. QI protects human umbilical vein endothelial cells from H_2O_2-induced cytotoxicity by evoking autophagy-induced Nrf2 nuclear translocation. (A) LC3B-I/LC3B-II and (B) Atg5/Atg13 protein levels examined by western blot analysis to determine the effect of QI on autophagy. LC3B-II levels were also examined by western blot analysis in (C) cells that were separately treated with CQ (10 μM) or QI (250 μM), or cotreated with both for 3 h, or (D) cells that were treated with QI (62.5, 125 and 250 μM) alone or with NAC (5 mM) pre-treatment for 1 h. (E) Confocal images obtained by immunohistochemical assay (blue, DAPI; green, Nrf2; scale bar, 10 μm), demonstrating the Nrf2 nuclear transfer following pretreatment with 3-MA (an autophagy inhibitor). (F) Cell viability determined by MTT assay in cells pretreated with 3-MA, followed by QI treatment. All assays were performed in triplicate, and data represent the mean ± standard deviation. **P<0.01, as indicated. QI, Quercetin-3-O-α-L-rhamnopyranoside; Nrf2, nuclear factor erythroid 2-related factor 2; Atg, autophagy related; 3-MA, 3-methyladenine; CQ, chloroquine; NAC, *N*-acetyl-L-cysteine.

which is then converted to water by catalase and GSH peroxidase (25). The results of the present study revealed that QI alleviated the H_2O_2-induced decrease in SOD activity and GSH content in HUVECs, suggesting that the cytoprotective effect of QI is likely associated with the restoration of endogenous antioxidation and the decrease of lipid peroxidation. This effect was also verified in aging rats, which were considered as a suitable model in the current study since the amount and activity of antioxidant enzymes in the body decrease with age, causing an increase in reactive oxygen and thus leading to a decline in physical function and various diseases. Aging rats undergoing QI treatment displayed improved SOD activity and greater GSH levels in the sera and heart tissues, as compared with the vehicle control. The MDA concentration was also

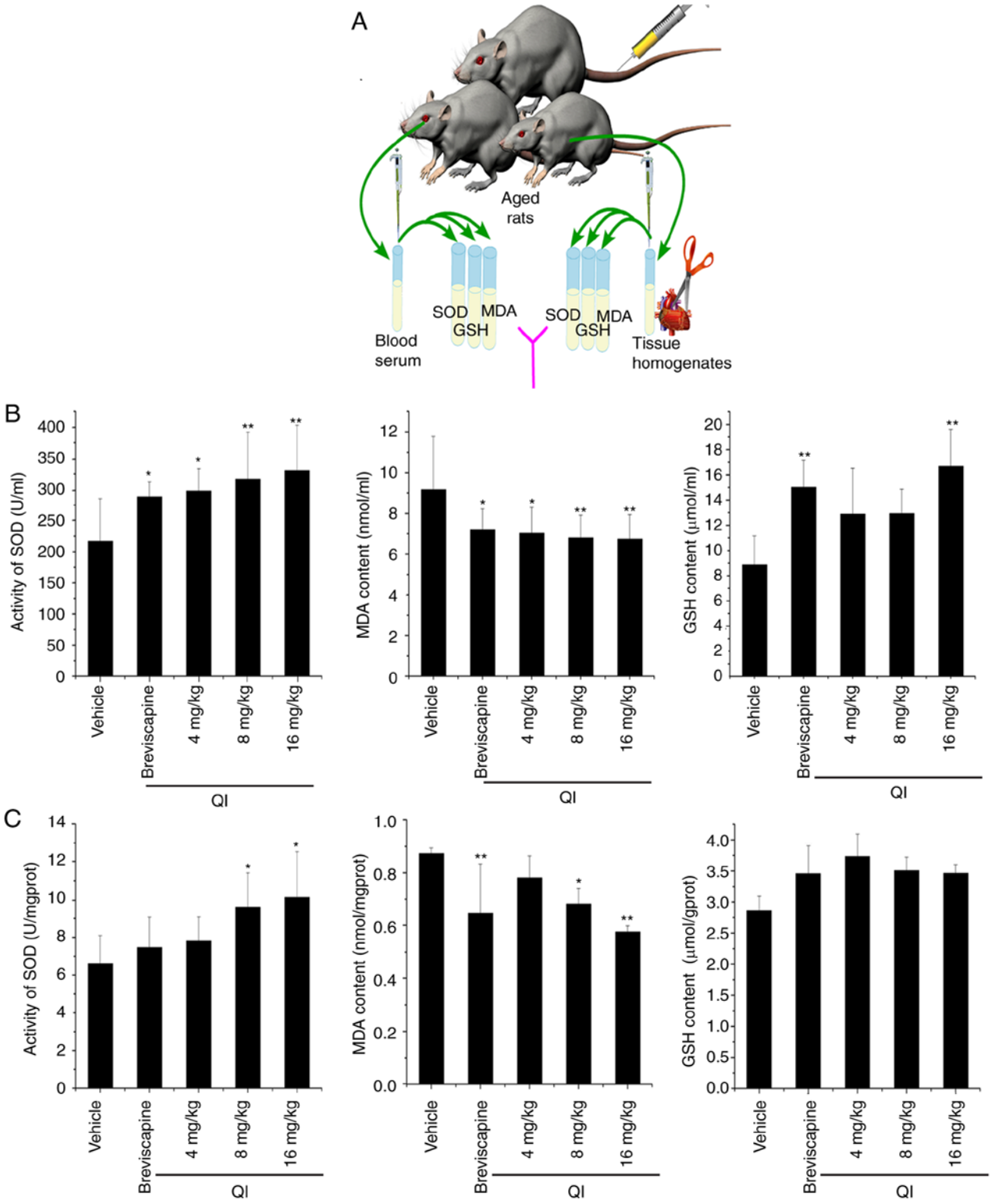

Figure 8. QI improves the activities of SOD and GSH, and decreases MDA content in the sera and heart tissues of aging rats. (A) Diagram of the animal experiment. All treatments were administered by tail vein injection once daily for two weeks. (B) Sera and (C) heart tissue homogenates were used to detect biochemical parameters associated with oxidative stress, including SOD, GSH and MDA, according to the protocols of the respective kits. Data represent the mean ± standard deviation. *P<0.05 and **P<0.01 vs. vehicle group. QI, Quercetin-3-O-α-L-rhamnopyranoside; SOD, superoxide dismutase; GSH, glutathione; MDA, malondialdehyde.

reduced in QI-treated cells and rats, confirming that QI improves the ability of endogenous antioxidation.

Excessive production of ROS in cells can directly and indirectly cause mitochondrial dysfunction, apoptosis and cell death (26). Nrf2 target genes are involved in the elimination of ROS (27). Therefore, Nrf2 is a potent transcriptional activator that serves a central role in the expression of several cytoprotective genes in response to oxidative stress (4). It was recently reported that the autophagy pathway maintains the integrity of the Keap1/Nrf2 pathway for normal liver function

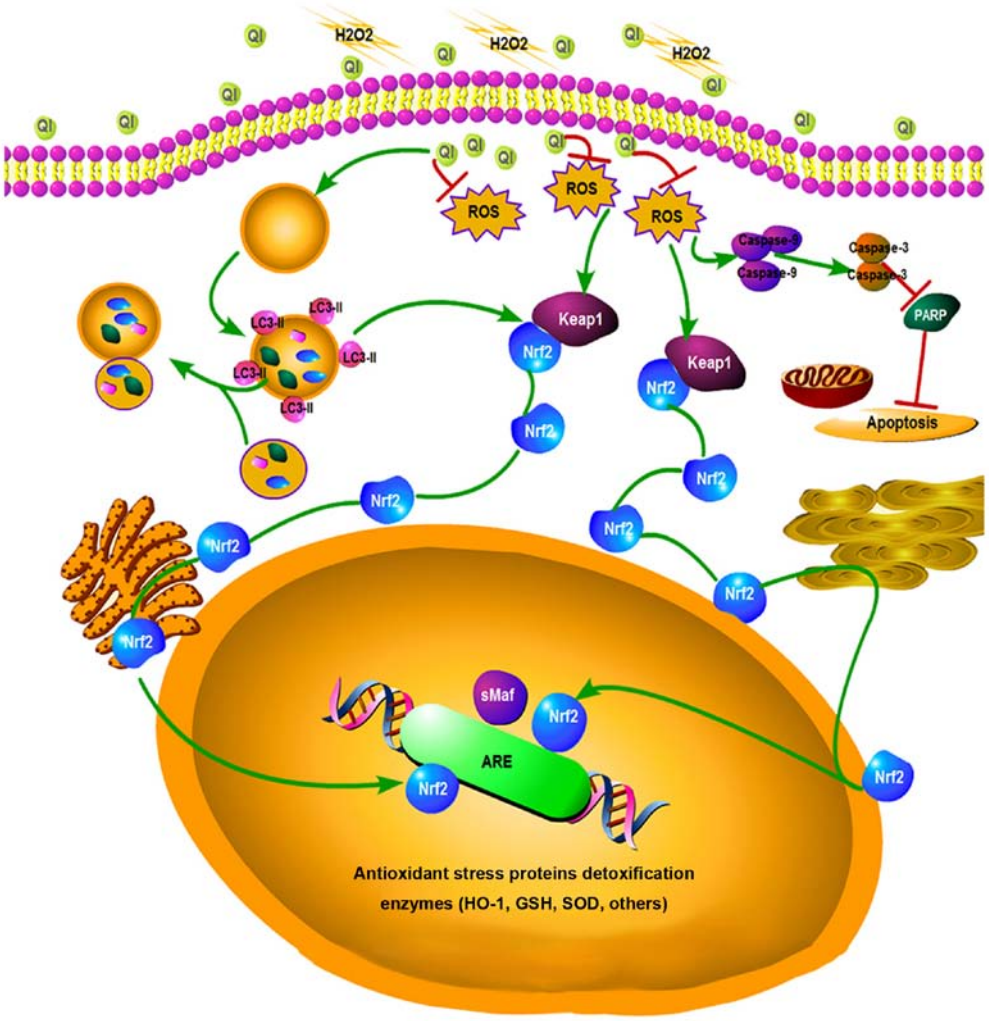

Figure 9. Diagram of the whole pathway. QI elicits significant autophagy for Nrf2 activation and Nrf2-dependent induction of major cellular antioxidant enzymes, and effectively attenuates H_2O_2-induced oxidative stress in human umbilical vein endothelial cells. QI, Quercetin-3-O-α-L-rhamnopyranoside; Nrf2, nuclear factor erythroid 2-related factor 2; ROS, reactive oxygen species; LC, light chain; Keap1, Kelch-like ECH-associated protein 1; PARP, poly(ADP-ribose) polymerase; ARE, antioxidant response element; HO-1, heme oxygenase-1; GSH, glutathione; SOD, superoxide dismutase.

by governing Keap1 turnover and that Nrf2 accumulation is the dominant cause of liver damage in autophagy-deficient mice (28). Additionally, autophagy is an effective protector of the inner ear against oxidative stress (8). To elucidate the underlying mechanism of these antioxidant effects, the expression levels of relevant proteins were measured in H_2O_2-damaged HUVECs following QI treatment in the present study. Treatment with QI inhibited the activation of Caspase-9, cleaved Caspase-3, and cleaved PARP, demonstrating that QI protects HUVECs from damage resulting from H_2O_2-mediated apoptosis. Immunofluorescence imaging and western blot analysis demonstrated the transfer of Nrf2 protein from the cytoplasm to the nucleus following QI treatment. Furthermore, transfection of cells with Nrf2 siRNA resulted in attenuation of the cytoprotective effect of QI. It is, thus, speculated that Nrf2 regulation is the critical cause of the antioxidant properties of QI.

Atg5 is E3-like activity for Atg8s-lipidaton and is required for autophagosome formation, while Atg13 is a member of the Atg1-Atg13-Atg17-Atg29 complex and is critical for correct localization of ULK1 to the pre-autophagosome and stability of ULK1 protein (29). Following QI treatment in the current study, Atg5, Atg13 and LC3B-II levels were upregulated, suggesting that QI promotes autophagy. This was further confirmed using 3-MA to study whether autophagy was involved in the protective mechanism. It was observed that pretreatment with 3-MA attenuated the protective effect of QI and inhibited the nuclear transfer of Nrf2, suggesting that QI protects HUVECs and activates the Nrf2 pathway by inducing autophagy. Further analysis demonstrated that the antioxidant effect of QI also occurs at the transcriptional level.

In conclusion, the current study provided evidence that QI elicits significant autophagy by Nrf2 activation and Nrf2-dependent induction of major cellular antioxidant enzymes, and effectively attenuates H_2O_2-induced oxidative stress in HUVECs (Fig. 9). These observations demonstrate the importance of the QI/autophagy/Nrf2 axis in the cellular response to oxidative stress-induced cell death and suggest that this axis may be a potential therapeutic target for oxidative stress-induced diseases.

Acknowledgements

Not applicable.

Funding

The present study was supported by Zhejiang Provincial Science and Technology Planning Project (grant no. 2016C04005), the Jiangsu Provincial Natural Science Foundation of China (grant no. BK20161269) and the National Science Foundation of China (grant no. 81473182).

Availability of data and materials

The datasets used and/or analyzed during the current study are available from the corresponding author on reasonable request.

Authors' contributions

HH and LZ designed the study. HH, BX and AA performed the *in vitro* experiments. HH, XY, HL and MG conducted the *in vivo* experiments. HH and AA analyzed the data and wrote the manuscript. All authors read and approved the final manuscript.

Ethics approval and consent to participate

All experimental procedures using live animals were conducted in accordance with protocols approved by the Ethics Review Committee for the Use of Animal Subjects of Zhejiang University (Zhejiang, China).

Patient consent for publication

Not applicable.

Competing interests

The authors declare that they have no competing interests.

References

1. Finkel T and Holbrook NJ: Oxidants, oxidative stress and biology of ageing. Nature 408: 239-247, 2000.
2. Rahman T, Hosen I, Islam MM and Shekhar HU: Oxidative stress and human health. Adv Biosci Biotechnol 3: 997-1019, 2012.
3. Birben E, Sahiner UM, Sackesen C, Erzurum S and Kalayci O: Oxidative stress and antioxidant defence. World Allergy Organ J 5: 9-19, 2012.
4. Motohashi H and Yamamoto M: Nrf2-Keap1 defines a physiologically important stress response mechanism. Trends Mol Med 10: 549-557, 2004.
5. Dhakshinamoorthy S, Jain AK, Bloom DA and Jaiswal AK: Bach1 competes with Nrf2 leading to negative regulation of the antioxidant response element (ARE)-mediated NAD(P)H: Quinone oxidoreductase 1 gene expression and induction in response to antioxidants. J Biol Chem 280: 16891-16900, 2005.
6. Chen S, Tang Y, Qian Y, Chen R, Zhang L, Wo L and Chai H: Allicin prevents H_2O_2-induced apoptosis of HUVECs by inhibiting an oxidative stress pathway. BMC Complement Altern Med 14: 321, 2014.
7. Maiuri MC, Zalckvar E, Kimchi A and Kroemer G: Self-eating and self-killing: Crosstalk between autophagy and apoptosis. Nat Rev Mol Cell Biol 8: 741-752, 2007.
8. Hayashi K, Dan K, Goto F, Tshuchihashi N, Nomura Y, Fujioka M, Kanzaki S and Ogawa K: The autophagy pathway maintained signaling crosstalk with the Keap1-Nrf2 system through p62 in auditory cells under oxidative stress. Cell Signal 27: 382-393, 2015.
9. Kim JA, Jung YS, Kim MY, Yang SY, Lee S and Kim YH: Protective effect of components isolated from Linderaerythrocarpa against oxidative stress-induced apoptosis of H9c2 cardiomyocytes. Phytother Res 25: 1612-1617, 2011.
10. Yu YB, Miyashiro H, Nakamura N, Hattori M and Park JC: Effects of triterpenoids and flavonoids isolated from Alnus firma on HIV-1 viral enzymes. Arch Pharm Res 7: 820-826, 2007.
11. Boppana K, Dubey PK, Jagarlapudi SA, Vadivelan S and Rambabu G: Knowledge based identification of MAO-B selective inhibitors using pharmacophore and structure based virtual screening models. Eur J Med Chem 44: 3584-3590, 2009.
12. Jang DS, Kim JM, Kim J, Yoo JL, Kim YS and Kim JS: Effects of compounds isolated from the fruits of Rumex japonicas on the protein glycation. Chem Biodivers 5: 2718-2723, 2008.
13. Choi B, Bae JY, Kim DS, Li J, Kim JL, Lee YJ and Kang YH: Dietary compound quercitrindampents VEGF induction and PPAR gamma activation in oxidized LDL-exposed murine macrophages: Association with scavenger receptor CD36. J Agric Food Chem 58: 1333-1341, 2010.
14. Hubert DJ, Dawe A, Florence NT, Gilbert KD, Angele TN, Buonocore D, Finzi PV, Vidari G, Bonaventure NT, Marzatico F and Paul MF: In vitro hepatoprotective and antioxidant activities of crude extract and isolated compounds from Ficusgnaphalocarpa. Inflammonpharmacology 19: 35-43, 2011.
15. Zhi K, Li M, Bai J, Wu Y, Zhou S, Zhang X and Qu L: Quercitrin treatment protects endothelial progenitor cells from oxidative damage via inducing autophagy through extracellular signal-regulated kinase. Angiogenesis 19: 311-324, 2016.
16. Xu C, Yang B, Zhu W, Li X, Tian J and Zhang L: Characterisation of polyphenol constituents of Linderae aggregata leaves using HPLC fingerprint analysis and their antioxidant activities. Food Chem 186: 83-89, 2015.
17. Ning L, Wentworth L, Chen H and Weber SM: Down-regulation of Notch1 signaling inhibits tumor growth in human hepatocellular carcinoma. Am J Transl Res 1: 358-366, 2009.
18. Choi HI, Kim HJ, Park JS, Kim IJ, Bae EH, Ma SK and Kim SW: PGC-1α attenuates hydrogen peroxide-induced apoptotic cell death by upregulating Nrf-2 via GSK3β inactivation mediated by activated p38 in HK-2 cells. Sci Rep 7: 4319-4331, 2017.
19. Li W, Ma F, Zhang L, Huang Y, Li X, Zhang A, Hou C, Zhu Y and Zhu Y: S-Propargyl-cysteine exerts a novel protective effect on methionine and choline deficient diet-induced fatty liver via Akt/Nrf2/HO-1 pathway. Oxid Med Cell Longev 2016: 4690857, 2016.
20. Livak KJ and Schmittgen TD: Analysis of relative gene expression data using real-time quantitative PCR and the 2(-Delta Delta C(T)) method. Methods 25: 402-408, 2001.
21. Li XL, Li YQ, Yan WM, Li HY, Xu H, Zheng XX, Guo DW and Tang LK: A study of the cardioprotective effect of breviscapine during hypoxia of cardiomyocytes in vitro and during myocardial infarction in vivo. Planta Medica 70: 1039-1044, 2004.
22. Gao Y, Chu S, Shao Q, Zhang M, Xia C, Wang Y, Li Y, Lou Y, Huang H and Chen N: Antioxidant activities of ginsenoside Rg1 against cisplatin-induced hepatic injury through Nrf2 signaling pathway in mice. Free Radic Res Commun 51: 1-13, 2017.
23. Hadi H, Carr CS and Suwadi JA: Endothelial dysfunction: Cardiovascular risk factors, therapy, and outcome. Vasc Health Risk Manag 1: 183-198, 2005.
24. Lum H and Roebuck KA: Oxidant stress and endothelial cell dysfunction. Am J Physiol Cell Physiol 280: C719-C741, 2001.
25. Zhai L, Zhang P, Sun RY, Liu XY, Liu WG and Guo XL: Cytoprotective effects of CSTMP, a novel stilbene derivative, against H_2O_2-induced oxidative stress in human endothelial cells. Pharmacol Rep 63: 1469-1480, 2011.
26. Kir HM, Dillioglugil MO, Tugay M, Eraldemir C and Özdoğan HK: Effects of vitamins E, A and D on MDA, GSH, NO levels and SOD activities in 5/6 nephrectomized rats. Am J Nephrol 25: 441-446, 2005.
27. Sugawara T and Chan PH: Reactive oxygen radicals and pathogenesis of neuronal death after cerebral ischemia. Antioxid Redox Signal 5: 597-607, 2003.
28. Yates MS, Tran QT, Dolan PM, Osburn WO, Shin SN, McCulloch CC, Silkworth JB, Taguchi K, Yamamoto M, Williams CR, *et al*: Genetic versus chemoprotective activation of Nrf2 signaling: Overlapping yet distinct gene expression profiles between Keap1 knockout and triterpenoid-treated mice. Carcinogenesis 30: 1024-1031, 2009.
29. Shibutani ST and Yoshimori T: A current perspective of autophagosome biogenesis. Cell Res 24: 58-68, 2014.